Engineered Science
DOI: https://dx.doi.org/10.30919/es1335

# Effect of Temperature During Laser Welding of Tissue Between Bioheat Model and Porous Media Model by Varying 3 Pattern of Laser Movement: Single-Line, Line and Zigzag

Totsaphon Chabuanoi,[1] Nattadon Pannucharoenwong,[1,*] Phanuwat Wongsangnoi,[2,*] Snunkhaem Echaroj,[1,*] Phadungsak Rattanadecho,[1] Jedsadakorn Saemathong,[1] Direk Nualsing[1] and Suphasit Panvichien[3]

## Abstract

This research investigates the development of a pulsed laser wound welding model using numerical calculations based on the finite element method. The study examines three movement patterns: Line, Zigzag, and Single-line. The study compares the Bioheat and Porous media models to examine the thermal effects during laser tissue welding and assess the accuracy of both models. The results indicate that, when changing the movement pattern, the Single-line movement generates the highest welding temperature, followed by the Line pattern, with the Zigzag pattern resulting in the lowest temperature. However, the temperature distribution in the Zigzag pattern is the most variable, followed by the Line and Single-line patterns, respectively. When comparing the accuracy of the Bioheat and Porous media models with experimental results from animal tissue samples that are comparable to human skin, the Porous media model demonstrated closer alignment with the actual experimental data than the Bioheat model. Nonetheless, while the animal tissue samples are similar to human tissue, they lack the blood circulation present in living human tissue. In the future, comparing the results obtained from human tissue studies will enhance the accuracy of the model. Furthermore, investigating how variations in pulse waveform affect the temperature during laser tissue welding should be a focus of future research to improve model accuracy and its applicability for real treatment planning.

*Keywords:* Laser moving; Laser welding skin tissue; Porous media model; Laser pulse; Thermal simulation.
Received: 14 October 2024; Revised: 20 November 2024; Accepted: 24 November 2024.
Article type: Research article.

## 1. Introduction

Wound healing with minimal scar formation has gained increasing importance in the medical and surgical fields. Scarring results from excessive granulation tissue formation during the healing process. Suturing is a popular method for wound closure due to its low cost, simplicity, and speed. However, it has drawbacks, including increased inflammation in surrounding tissues, leading to larger-than-necessary scars, and it is not feasible for very narrow areas.

The use of lasers for wound welding has begun to gain popularity in research as a potential future treatment method. Laser wound weld involves applying laser energy to the tissue to generate heat, which subsequently stimulates the tissue to produce proteins that facilitate wound adhesion. This method offers several advantages, including faster healing, reduced inflammation, and less scar formation compared to traditional suturing techniques.

The technique of laser wound weld has been tested on animal tissue samples, such as porcine skin, using various treatment methods, yielding results that closely resemble human tissue. However, these findings cannot be directly compared to outcomes in human skin due to the lack of blood circulation in the animal tissue samples, as well as differences in tissue temperature from actual human skin.[1-4] Additionally,

[1] *Department of Mechanical Engineering, Faculty of Engineering, Thammasat School of Engineering, Thammasat University, Bangkok, 12120, Thailand*
[2] *Department of Mechanical and Industrial, Faculty of Industrial Technology, Sakon Nakhon Rajabhat University, Sakon Nakhon, 47000, Thailand*
[3] *School of Biomedical Engineering & Imaging Sciences, Faculty of Life Sciences & Medicine King's College London, London, WC2R 2LS, United Kingdom*
**Email:* pnattado@engr.tu.ac.th (N. Pannucharoenwong), wongsangnoi@hotmail.com (P. Wongsangnoi), snunkha@engr.tu.ac.th (S. Echaroj)

experiments using lasers on laboratory mice have shown promising results, but the application of these methods to human treatment is still not feasible, as the tissue properties in animal models differ from those in humans, and there is a lack of diversity in the experimental subjects.[5-12]

Another approach that closely resembles the actual condition of human skin tissue involves using finite element methods to create computer models of human skin. These models simulate the real conditions of human tissue and the patterns of heat distribution when heated by a thermal source. Most modeling is conducted under the Bioheat theory proposed by Pennes, which simulates blood flow throughout the tissue.[13] While this method has proven effective, it still does not closely approximate actual human tissue as it could be.[14-22] The physical characteristics of real tissues are composed of cells and glands within the skin layer. Blood flow results in particle interactions within the tissue and facilitates heat exchange. Consequently, modeling using Porous media theory has begun to be applied to create more accurate models of human tissue, yielding results that are closer to actual human skin than those produced by the Bioheat model. The Porous media theory has been utilized in simulations for various human organ treatments;[23-28] however, it has yet to be applied to modeling laser wound weld. If this technique were adapted to create a model for laser wound weld, it would enhance the accuracy of the simulations. Additionally, several research studies have developed moving laser models to increase the diversity of simulations, making them more representative of real treatment scenarios.[29-32] Nevertheless, previous studies have not simulated treatments with a moving laser by creating a skin tissue model as Porous material. A recent study developed a Bioheat model for laser tissue welding to investigate the thermal effects of varying the speed and size of the laser used for wound closure. The results indicated that increasing the laser speed and reducing its size resulted in higher temperatures at the wound site. These findings should be further explored to enhance the model's accuracy in comparison to actual treatment outcomes by incorporating a comparative analysis with the Porous media model. Additionally, expanding the study to include various laser movement patterns could improve the versatility and applicability of the treatment methods.[33]

The biological structure of human skin tissue is composed of numerous glands and cells, which are regarded as a solid phase, and it also contains the surrounding blood, which is regarded as a liquid phase. Simulating the biological characteristics of skin tissue to closely resemble actual human tissue is crucial for accurately predicting temperature effects in studies. In laser wound welding techniques, the maximum temperature generated must not exceed 65 °C, as higher temperatures can damage the tissue. The model based on Porous Media theory has been compared with previously studied Bioheat theory models. The Porous media theory provides a more accurate representation of the biological structure of human skin. It is essential to investigate the resulting maximum temperature and the temperature distribution during treatment. When comparing the laser wound welding models based on Bioheat theory and Porous media theory, determining which model yields results more closely aligned with actual experimental outcomes is critical for improving predictive accuracy in computer-based modeling of treatments. Furthermore, actual wounds exhibit varying characteristics; altering the laser movement patterns may enhance temperature distribution throughout the tissue during laser healing. This could potentially lower the maximum temperature to appropriate levels, preventing thermal damage to the tissue. Investigating the actual temperature outcomes in these studies is imperative. If successful, the findings would significantly benefit the medical field, enabling physicians to plan treatments more accurately and potentially reducing healthcare costs.

This research aims to develop a model of human skin tissue using the finite element method to create a computer simulation. The results of this simulation will be compared between models based on the Bioheat theory and Porous media theory, using experimental data from actual tissue samples obtained from laboratory animals. The goal is to determine which theoretical framework provides results for laser wound welding that closely align with actual laboratory experiments. Additionally, the study involves altering the laser pulse movement patterns from a single-line approach over the wound area to zigzag and line patterns. This modification aims to compare the heat distribution and the resulting maximum temperatures. If the temperatures exceed 65 °C, the skin tissue may be damaged due to heat. Conversely, if the temperatures are too low, it could result in inadequate tissue bonding.[34] The studied parameters are shown in Table 1 and Table 2.

**Table 1.** Laser parameters.

| Welding parameters | Symbols | Unit | values |
|---|---|---|---|
| Laser Power | P | W | 10 |
| Welding speed | v | m/s | 0.1 |
| Spot radius | ρ | mm. | 0.3 |
| Welding time | t | s | 1 |
| Pulse frequency | f | kHz | 10 |
| Pulse duration | | ns | 0.01 |

## 2. Experimental section

### 2.1 Mathematical model

This study compares the maximum temperatures generated during laser welding by altering the movement patterns in three configurations: single-line, zigzag, and line. The 3D mathematical model developed includes two layers of skin: the epidermis and the dermis, as illustrated in Fig. 1. This figure shows the actual tissue layers of the skin, resembling porous materials, with the epidermis and dermis having thicknesses of 0.05 mm and 1.95 mm, respectively. A pulsed laser serves as the heat source, and the study investigates the thermal field when modifying the tissue layer modeling using both Bioheat theory and Porous media theory.

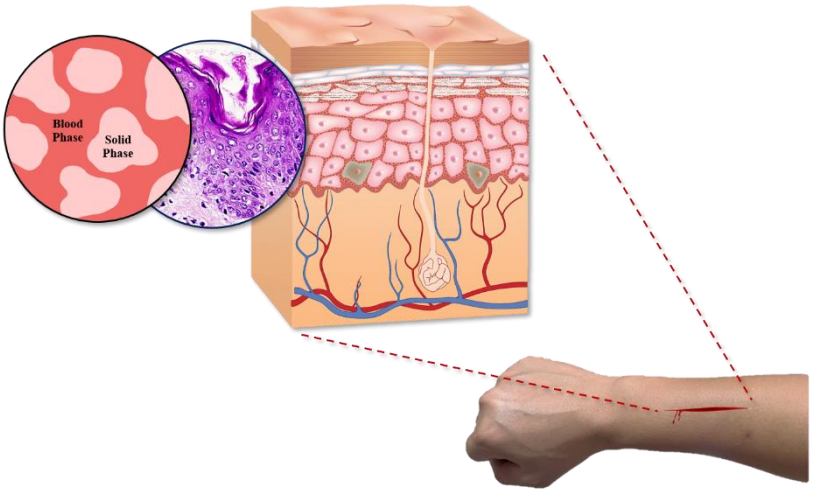


**Fig. 1** Porous media layer of the skin tissue.

**Table 2.** Thermal properties, optical properties, and physical properties of tissue and blood.[35-41]

| Properties | Symbols | Unit | Epidermis | Demis |
|---|---|---|---|---|
| Thickness | Z | mm. | 0.05 | 1.95 |
| Tissue density | $\rho$ | kg/m$^3$ | 1,200 | 1,200 |
| Specific heat of tissue | $C_p$ | J/kg·K | 3,600 | 3,800 |
| Thermal conductivity of tissue | K | W/(m·K) | 0.21 | 0.53 |
| Absorption coefficient | $\alpha$ | 1/m | 2,000 | 240 |
| Scattering coefficient | $\beta$ | 1/m | 47,000 | 12,900 |
| Ambient temperature | $T_m$ | ℃ | 25 | |
| Initial temperature | $T_0$ | ℃ | 36 | 36 |
| Blood perfusion | $w_b$ | 1/s | 0 | 0.0031 |
| Blood temperature | $T_b$ | ℃ | 36 | |
| Blood density | $\rho_b$ | kg/m$^3$ | 1,058 | |
| Specific heat of blood | $C_b$ | J/kg·K | 3,960 | |
| Thermal conductivity of blood | $K_b$ | W/m·K | 0.45 | |
| Heat convection coefficient | h | W/m$^2$·K | 10 | |

### 2.2 Modeling skin tissue

Human skin tissue consists of three primary layers. The outermost layer, known as the epidermis, is characterized by a constant turnover of cells, with new cells being produced while older ones shed from the body. This layer contains numerous hair follicles, sebaceous glands, and sweat glands. The second layer, referred to as the dermis, comprises skin cells, lymphatic glands, nerve endings, hair root follicles, muscles, and a rich network of blood vessels. The innermost layer is the subcutaneous fat, which primarily consists of fat cells and varies in thickness among individuals, providing insulation to the body.

This research constructs a three-dimensional model of skin tissue divided into two layers: the epidermis and the dermis. The epidermis is modeled with a thickness of 0.05 mm, while the dermis has a thickness of 1.95 mm. However, the subcutaneous fat layer is not included in the model due to its considerable depth and negligible effect on external heat absorption. The properties of the tissue are shown in Table 2. The model dimensions are 20 × 20 mm, with the laser moving along the wound axis in the X-direction. The model developed under the Bioheat theory simulates the entire tissue as being fully surrounded by a liquid (blood), while the model based on Porous media theory simulates the solid tissue interspersed within spaces filled with liquid (blood). This approach is reflective of the actual structure of human skin tissue, which consists of a complex arrangement of cells and fluids, as depicted in Fig. 2.

### 2.3 Heat transfer analysis

The heat transfer from a laser, which serves as the heat source, to the skin tissue and the subsequent heat distribution across various skin layers must pass through tissues with differing thermal properties. The process is further influenced by blood circulation, which acts as a mechanism for convective heat transfer to other parts of the tissue, as well as by the intercellular space, which has its own distinct thermal characteristics. These factors collectively affect the efficiency of heat conduction and the temperature generated during tissue welding with laser-induced heat.

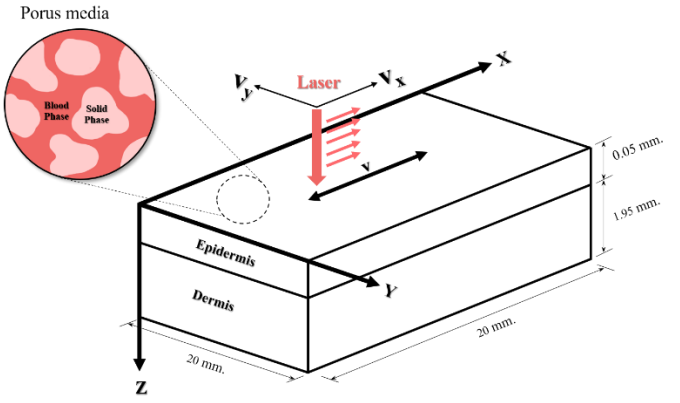


**Fig. 2** Schematic diagram of laser moves on Porus media tissue model.

In this study, the laser heat source moves in various patterns along the X-axis, transmitting heat to the surface of the skin tissue. The uppermost layer of the tissue experiences convective heat transfer with the surrounding air at a constant rate of 10 W/mm². The ambient air temperature around the tissue is 25 °C, and the initial temperature of the tissue is 36 °C, as shown in Fig. 3. The following assumptions apply:

1. The thermal properties of the skin tissue are constant.
2. There is no phase change of the substances within the porous skin tissue.
3. No chemical reactions occur within the porous skin tissue.
4. The porous skin tissue is homogeneous and exhibits uniform heat distribution.

### 2.3.1 Bioheat equation

Computer modeling studies use the Bioheat modeling equations developed by Harry Pennes in 1948.[13] The equations describe heat transfer within tissues through blood flow, heat from external sources, and heat within the tissues due to metabolic processes, as shown in Eq. (1).

$$\rho C\frac{\partial T}{\partial t} = K\nabla^2 T + \rho_b C_b \omega_b (T_a - T_b) + Q_{met} + Q_r \quad (1)$$

where $\rho$ is density (kg/m³), $C$ is the heat capacity of tissue (J/kg·°C), T is the tissue temperature (°C), $K$ is the thermal conductivity (W/m·°C), $Q_{met}$ is the metabolic heat source within the tissue (W/m²), and $Q_r$ is the external heat source (W/m²).

### 2.3.2 Porous media equation

Porous materials generally consist of three states of matter: solid, liquid, and gas, which occupy the pore spaces. Based on the structure of porous materials, they can be categorized into two major types. In the first type, liquid or moisture moves around the solid particles (solid matrix) within the pore spaces, passing through without being absorbed by the solid particles. This type is known as non-hygroscopic porous media. In the second type, moisture is bound within the solid material through chemical and physical bonds, causing the moisture to remain stable within the structure. In this type of Porous media, the solid particles are very small, measuring between 0-1 nanometers. This type is referred to as hygroscopic Porus media.

#### 2.3.2.1 Energy equation

The thermal processes occurring within porous skin tissue are governed by a heat transfer equation in which the energy from the laser is absorbed into the tissue and combined with the energy within the tissue, causing the temperature within the porous skin tissue to increase.[42] The governing equation describing the heat transfer phenomenon is given by Eqs. (2)-(4).

$$(\rho C_p)_{eff}\frac{\partial T}{\partial t} + (\rho C_p)_b\left(u\frac{\partial T}{\partial r} + w\frac{\partial T}{\partial z}\right) = K_{eff}\left(\frac{\partial^2 T}{\partial r^2} + \frac{\partial^2 y}{\partial z^2}\right) + Q_{met} + Q_{ext} \quad (2)$$

$$(\rho C_p)_{eff} = (1\text{-}\varnothing)(\rho C_p)_s + \varnothing\,(\rho C_p)_b \quad (3)$$

$$K_{eff} = (1\text{-}\varnothing)K_s + \varnothing K_b \quad (4)$$

where $\varnothing$ is tissue porosity, $T$ is temperature (°C), $\rho$ is (kg/m³), K is thermal conductivity (W/m·°C), $C_p$ is specific heat capacity (J/kg· °C), subscripts eff is the effective value,

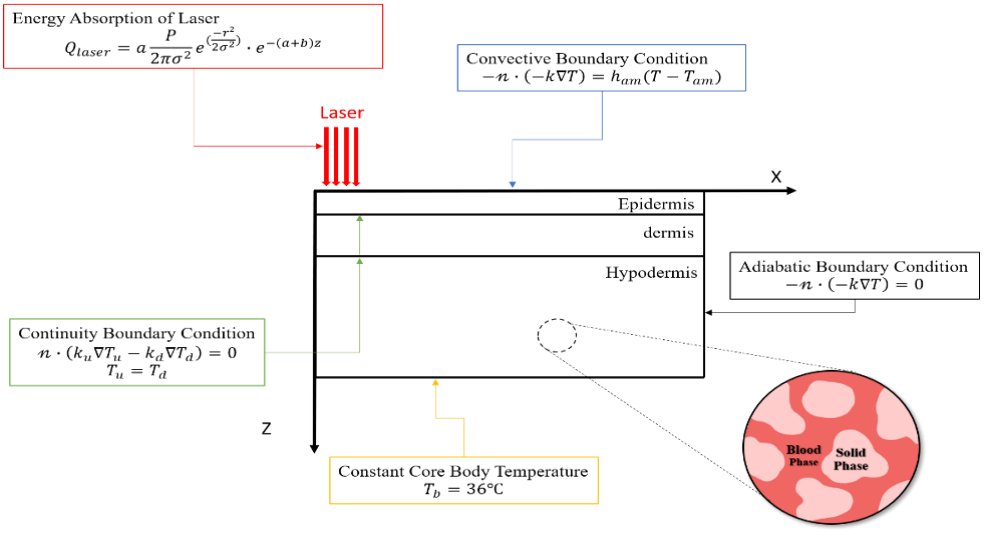


**Fig. 3** Boundary condition and the physical domain of Porus media modal.

subscripts *s* is the solid and subscripts *b* is the blood phase.

#### 2.3.2.2 Momentum equation

To describe the blood flow within porous tissue, the Brinkman flow equation model is used, along with the continuity Eq. (5) and the momentum Eqs. (6) and (7) to model blood flow in porous skin.[43]

$$\frac{\partial u}{\partial r}+\frac{\partial w}{\partial z}=0 \tag{5}$$

$$\frac{1}{\emptyset}\left[\frac{\partial u}{\partial t}\right]+\frac{1}{\emptyset^2}\left[u\frac{\partial u}{\partial r}+w\frac{\partial u}{\partial z}\right]=-\frac{1}{\rho_b}\left[\frac{\partial p}{\partial r}\right]+\frac{v}{\emptyset}\left[\frac{\partial^2 u}{\partial r^2}+\frac{\partial^2 u}{\partial z^2}\right]-\frac{uv}{k} \tag{6}$$

$$\frac{1}{\emptyset}\left[\frac{\partial w}{\partial t}\right]+\frac{1}{\emptyset^2}\left[u\frac{\partial w}{\partial r}+w\frac{\partial w}{\partial z}\right]=-\frac{1}{\rho_b}\left[\frac{\partial p}{\partial z}\right]+\frac{v}{\emptyset}\left[\frac{\partial^2 w}{\partial r^2}+\frac{\partial^2 w}{\partial z^2}\right]-\frac{uv}{k}+g\beta(T-T_\infty) \tag{7}$$

where $u$ and $w$ are blood velocity along the axis within the porous tissue (m/s), $p$ is pressure (Pa), $v = 3.78\text{x}10^{-7}$ m$^2$/s is the Kinematics viscosity, the coefficient of thermal expansion $\beta = 1\times10^{-4}$, 1/K is the coefficient of the thermal expansion, and $k$ is permeability (m$^2$) the following equation.[44]

$$k=\frac{\emptyset^3 d_p^2}{175(1-\emptyset)^2} \tag{8}$$

where $d_p = 1\times10^{-4}$ m$^2$ is the diameter of the cell.

From Eqs. (1) and (2) the external heat source ($Q_{ext}$) is a laser equation that uses Beer-Lambert law to create a heat source equation, where the heat generated in tissue depends on the optical properties of the tissue,[45] as shown in the Eq. (9).

$$Q_{ext}=aI_0e^{\left(\frac{-r^2}{2\sigma^2}\right)}\cdot e^{-\gamma z} \tag{9}$$

where $\gamma$ = a+b, *I (Z)* intensity in the z-direction (W/m$^2$), $I_0$ intensity incident light (W/m$^2$), $a$ is the absorption coefficient (1/m), $b$ is the scattering coefficient (1/m), $z$ the depth within the tissue (mm), and $\sigma$ is the radius of the laser beam in laser irradiation (mm).

#### 2.3.3 Energy from laser heat source

The energy of the laser beam distributed within the tissue layer at a depth along the direction z is equivalent to the laser power incident on the tissue surface area. That is,

$$P=2\pi I_0\sigma^2 \tag{10}$$

Substituting $P$ in Eq. (10) gives the heat source Eq. (11)

$$Q(r,z)=a\cdot\frac{P}{2\pi\sigma^2}\cdot e^{\left(\frac{-r^2}{2\sigma^2}\right)}\cdot e^{-(a+b)z} \tag{11}$$

where $P$ is a constant Power of laser (W).

The upper part of the skin layer loses heat by convection from the outside air at 25 (°C) as shown in Eq. (12)

$$-n\cdot(-k\nabla T)=h_{am}(T-T_{am}) \tag{12}$$

where $T_{am}$ is the ambient temperature (°C) and $h_{am}$ the ambient air heat transfer coefficient (W/m).

Each skin layer is closely connected with the others without any thermal resistance between the skin layers, as shown in Eqs. (13) and (14).[46]

$$n\cdot(k_u\nabla T_u-k_d\nabla T_d)=0 \tag{13}$$

$$T_u=T_d \tag{14}$$

### 2.4 Method

A computer model was developed using numerical simulation and analyzed with COMSO Multiphysics software to simulate skin tissue based on the Bioheat and Porous Media theories. The model consists of a total of 60,352 elements, as increasing the number of elements beyond this did not improve the accuracy of the model, as shown in Fig. 4. The movement of the laser was modified into three patterns: Line, Zigzag, and Single-line, with the laser motion patterns depicted in Fig. 5. The laser's position changes over time for each motion pattern, as shown in Table 3. The laser heat source is set to emit energy in the form of pulses, as illustrated in Fig. 6, with pulse parameters provided in Table 1. The simulation results were then compared with experimental data from

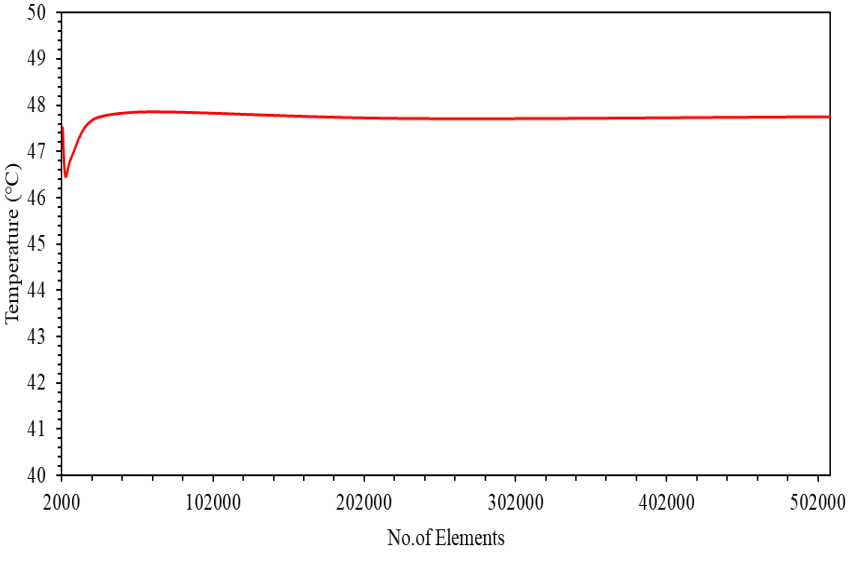


**Fig. 4** Mesh independence.

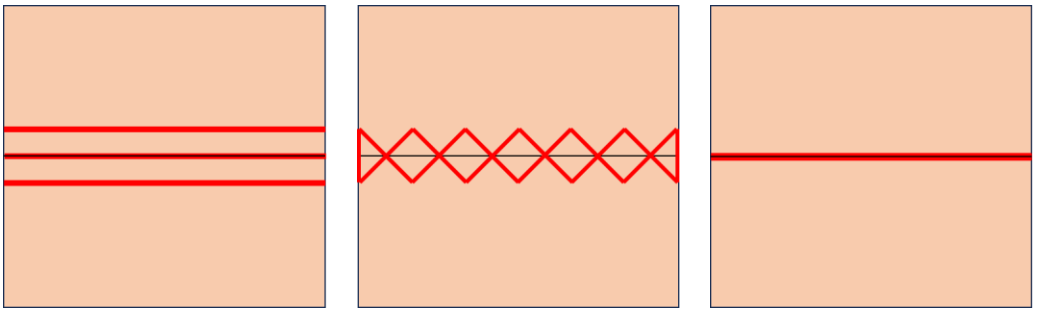

(a) (b) (c)

**Fig. 5** laser movement pattern (a) Line, (b) Zigzag, and (c) Single line.

**Table 3.** Laser movement position.

| Time(s) | X_line | Y_line | X_zigzag | Y_zigzag | X_single line | Y_single line |
|---|---|---|---|---|---|---|
| 0 | -10 | 1 | -10 | 1 | -10 | 0 |
| 0.01 | -9 | 1 | -9 | -1 | -9 | 0 |
| 0.02 | -8 | 1 | -8 | 1 | -8 | 0 |
| 0.03 | -7 | 1 | -7 | -1 | -7 | 0 |
| 0.04 | -6 | 1 | -6 | 1 | -6 | 0 |
| 0.05 | -5 | 1 | -5 | -1 | -5 | 0 |
| 0.06 | -4 | 1 | -4 | 1 | -4 | 0 |
| 0.07 | -3 | 1 | -3 | -1 | -3 | 0 |
| 0.08 | -2 | 1 | -2 | 1 | -2 | 0 |
| 0.09 | -1 | 1 | -1 | -1 | -1 | 0 |
| 0.1 | 0 | 1 | 0 | 1 | 0 | 0 |
| 0.11 | 1 | 1 | 1 | -1 | 1 | 0 |
| 0.12 | 2 | 1 | 2 | 1 | 2 | 0 |
| 0.13 | 3 | 1 | 3 | -1 | 3 | 0 |
| 0.14 | 4 | 1 | 4 | 1 | 4 | 0 |
| 0.15 | 5 | 1 | 5 | -1 | 5 | 0 |
| 0.16 | 6 | 1 | 6 | 1 | 6 | 0 |
| 0.17 | 7 | 1 | 7 | -1 | 7 | 0 |
| 0.18 | 8 | 1 | 8 | 1 | 8 | 0 |
| 0.19 | 9 | 1 | 9 | -1 | 9 | 0 |
| 0.2 | 10 | 1 | 10 | 1 | 10 | 0 |

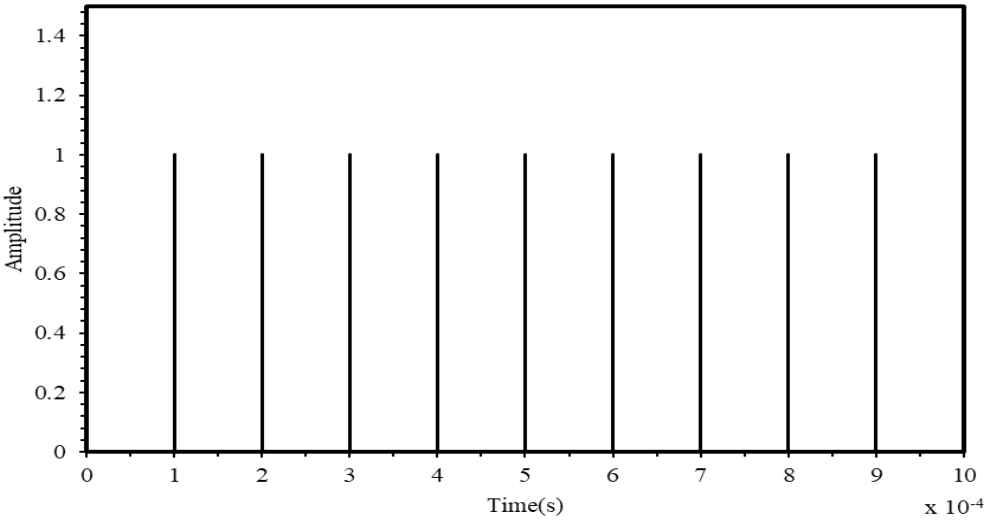


**Fig. 6** Laser pulse waveforms.

actual tissue samples to identify the model that most closely resembles real-world conditions and produces the optimal maximum temperature. The maximum temperature must not exceed 65 °C, as higher temperatures can cause tissue damage due to heat. The entire study process is shown in Fig. 7.

## 3. Results and discussion

### 3.1 Verification

The validation of the Bioheat modeling was carried out by comparing it with the work of Saemathong *et al.*[47] , who studied the use of lasers in dermatological treatments. By setting the same parameters, but without the movement of the laser, it was found that the results were comparable, as shown in Fig. 8. Subsequently, a comparison was made with the model by Ma *et al.*[48], Who also studied the use of a moving laser. It was found that the results were similarly close, with the differences attributed to the variation in laser shape, as illustrated in Fig. 9.

### 3.2 Temperature field

This section focuses on the temperature response of tissue during thermal welding using a pulsed laser heat source. The study analyzes the maximum temperature occurring during laser heating for two tissue models: the Bioheat model and the Porous media model. The temperature variation follows a pulsed pattern, as shown in Fig. 10, where the temperature increases in a stepwise manner corresponding to the on-off cycling of the laser. The laser parameters include a power of 10W, a laser movement speed of 100 mm/s, a pulse frequency of 10 kHz, a spot size of 0.6 mm, and a pulse duration of 0.01 ns. Three different laser movement paths were investigated: Line, Zigzag, and Single-line. The laser movement paths are illustrated in Fig. 5 and Table 3.

Figure 11 shows the laser trajectory at 0.9s during laser tissue bonding, Figs. 11(a)-(b) illustrates the laser movement in a Line pattern. Fig. 11(a) presents the model based on Bioheat theory, showing a maximum temperature of 62.3 °C. Fig. 11(b) depicts the Porous media model with a maximum temperature of 49.3 °C. The heat distribution is concentrated along the linear path of the laser movement and decreases as the laser shifts along the Y-axis. The Porous media model shows better temperature distribution than the Bioheat model. Figs. 11(c)-(d) illustrates the laser movement in a Zigzag

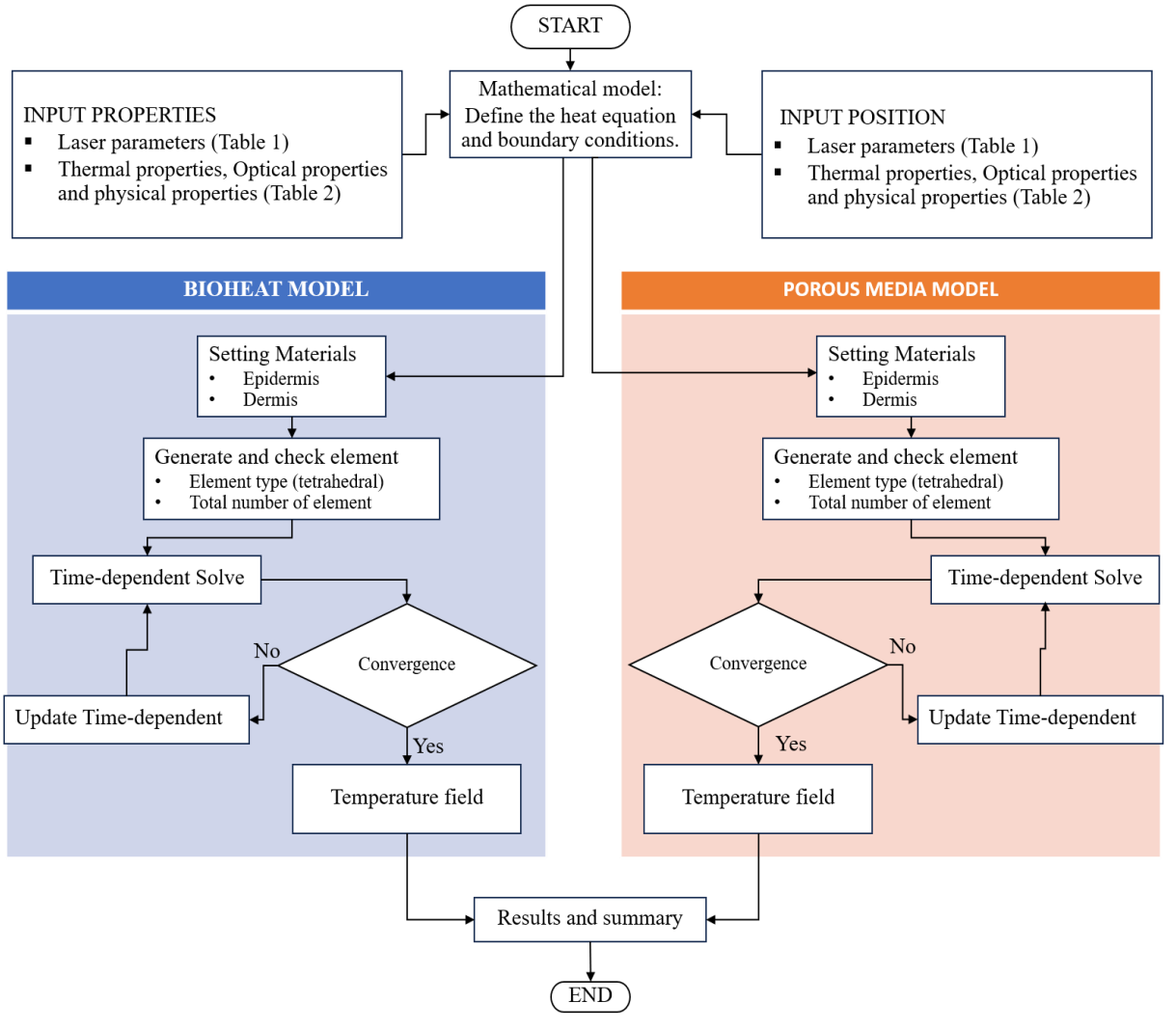


**Fig. 7** The flow diagram of calculation laser welding skin tissue.

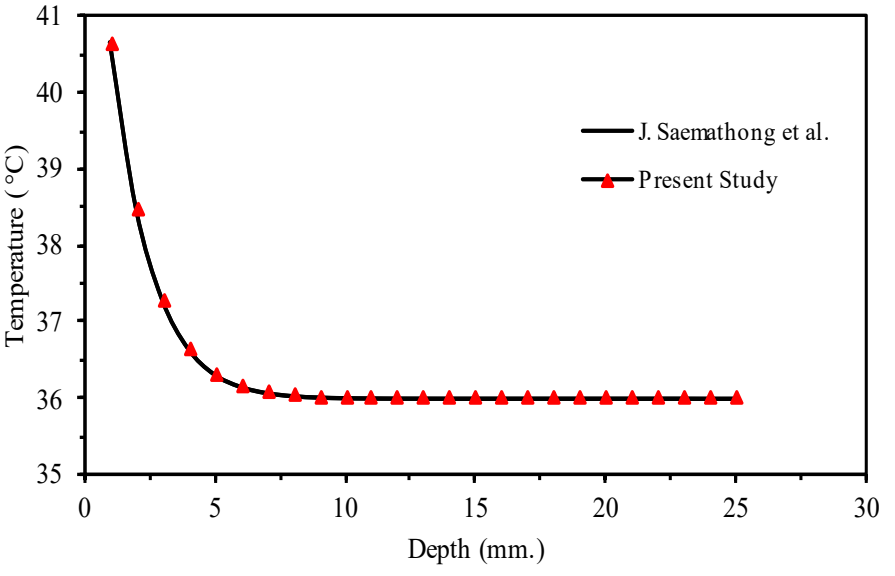


**Fig. 8** Comparison of the depth temperature distribution with the study of Saemathong *et al*.[47]

pattern. This movement results in the most extensive heat distribution across the tissue bonding area, with heat spreading evenly throughout the bonding zone. However, this movement pattern produces a lower maximum temperature compared to other methods, which may not be suitable for bonding processes that require higher heat. Fig. 11(c) represents the Bioheat model, while Fig. 11(d) shows the Porous media model. From the figures, it can be observed that thetemperature distributions are similar, but the Porous media model exhibits a smaller temperature range compared to the Bioheat model, and the maximum temperature is also lower in the Bioheat model. Figs. 11(e)-(f) depict single-line movement, where the laser travels directly over the incision. This type of movement reflects the traditional method of laser welding for incisions, which has been widely studied in the past. This movement pattern yields the highest temperatures,

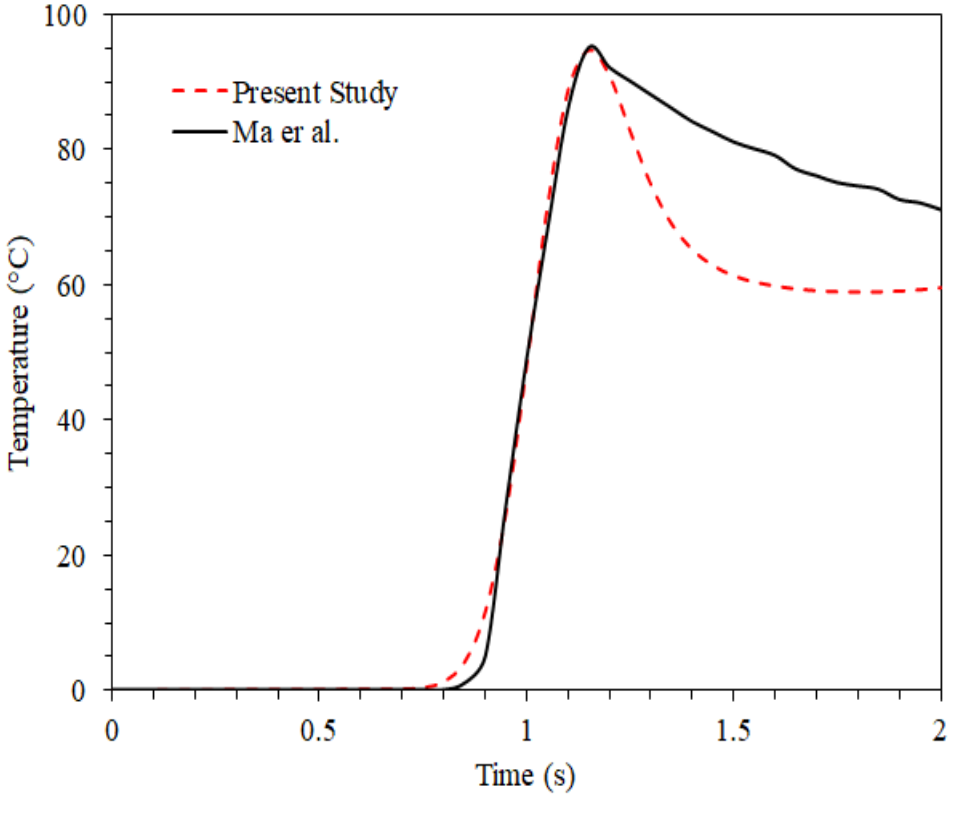


**Fig. 9** Comparison of the model with the research of Ma *et al*.[48]

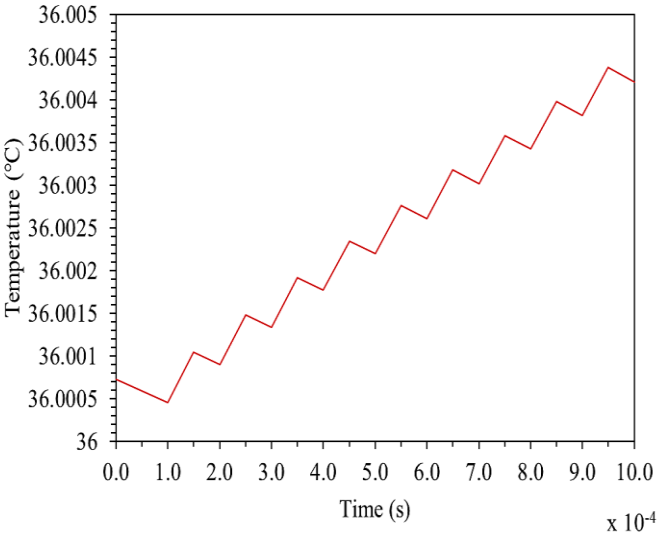


**Fig. 10** Temperature increases by pulsed laser.

with the Bioheat model reaching a maximum temperature of 69.2 °C as shown in Fig. 11(e), and the Porous media model reaching 51.6 °C as shown in Fig. 11(f). These temperatures are higher than those observed in other movement patterns. The heat distribution is concentrated along the straight line in the laser's path, making this movement pattern suitable for straight incisions without complex shapes. Both models show similar temperature distributions, but the Bioheat model exhibits higher temperatures than the Porous media model. Figure 12 shows the temperature distribution along the Y-axis of the tissue welded by a laser with line movement, comparing the Bioheat and Porous media models at position X = -4 mm at 0.9 seconds. It was found that the Bioheat model exhibited a higher maximum temperature at position Y = 1 mm compared to the Porous media model. Meanwhile, the region between X = 0 mm to X = -2 mm represents the temperature of the previously welded area that the laser has already passed over. The temperature gradient of the Porous media model is less steep than that of the Bioheat model, indicating that the Porous media model dissipates heat more effectively, resulting in a lower maximum temperature compared to the Bioheat model.

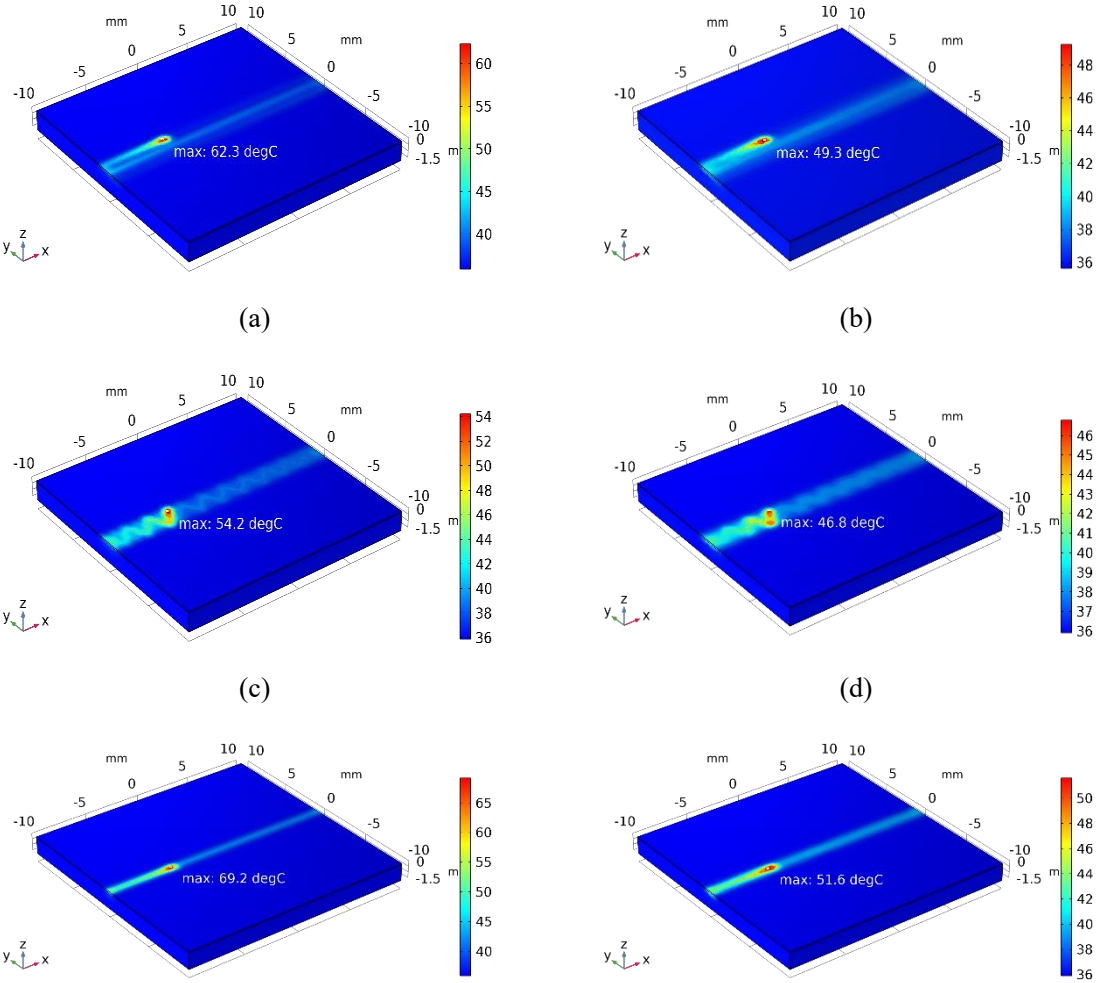


(a) (b) (c) (d) (e) (f)

**Fig. 11** compares the movement patterns of the Bioheat and Porous media models: (a) Bioheat model with a line movement pattern, (b) Porous media model with a line movement pattern, (c) Bioheat model with a zigzag movement pattern, (d) Porous media model with a zigzag movement pattern, (e) Bioheat model with a single-line movement pattern, and (f) Porous media model with a single-line movement pattern.

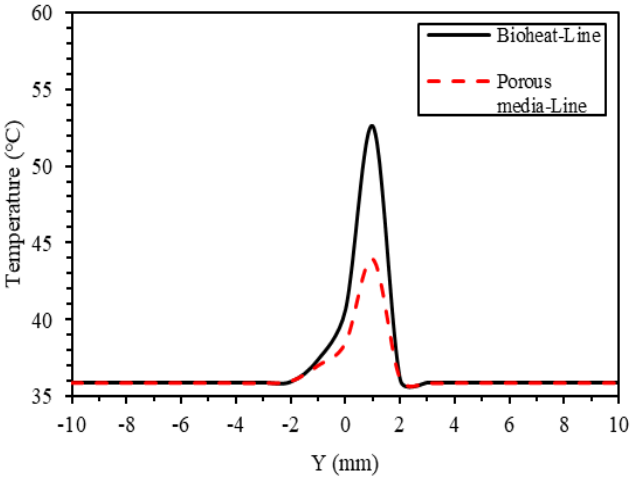


**Fig. 12** Temperature in the Y-axis when the laser moves in a Line pattern.

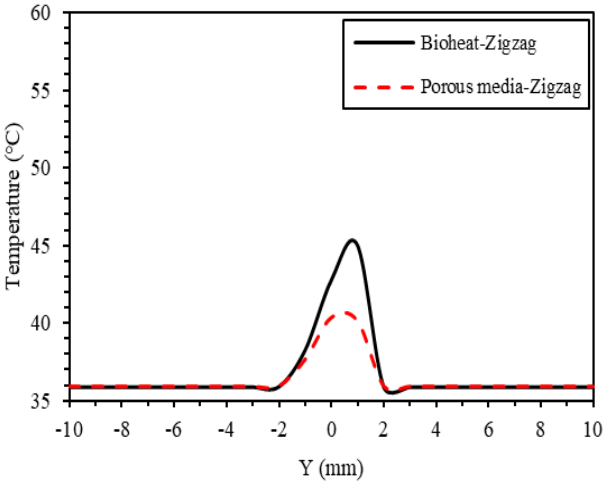


**Fig. 13** Temperature in the Y-axis when the laser moves in a Zigzag pattern.

Figure 13 shows the temperature distribution along the Y-axis during laser welding of tissue at position X = -4 mm at 0.9 seconds, where the laser moves in a zigzag pattern, comparing the Bioheat and Porous media models. It was found that at position Y = 1 mm, the Bioheat model exhibited a maximum temperature of 45 °C, which is higher than the Porous media model's maximum temperature of 40.3 °C at position Y = 0.5 mm. However, the Porous media model has a wider temperature distribution range, leading to less temperature variation in the surrounding area near the laser point compared to the Bioheat model.

Figure 14 shows the temperature profiles of the Bioheat and Porous media models when the laser moves in a single-line pattern, a traditional movement pattern widely studied in previous laboratory experiments. At position X = -4 mm and time 0.9s, it was found that the temperature distribution patterns were similar, as there was no change in the welding direction along the Y-axis, with the laser repeatedly moving along the same path at Y = 0 mm. However, the maximum temperature in the Bioheat model was higher than in the porous media model.

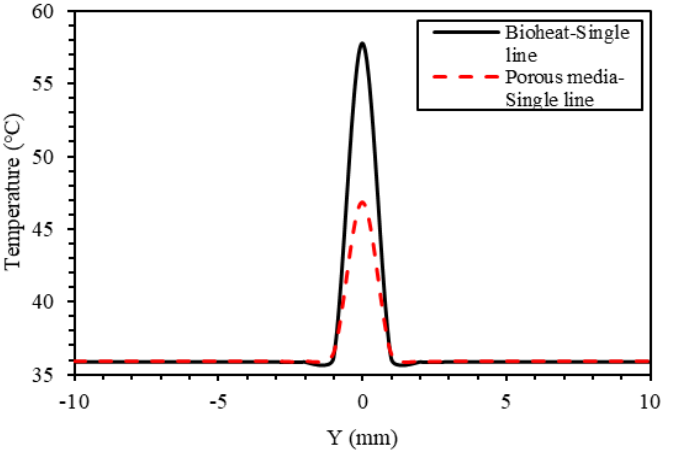


**Fig. 14** Temperature in the Y-axis when the laser moves in a Single line pattern.

Figure 15 compares the temperature along the Y-axis when using three different laser movement patterns, Line, Zigzag, and Single-line, for both the Bioheat and Porous media models. It was observed that the Bioheat model with Single-line movement generated the highest temperature compared to other patterns, while the Porous media model with Zigzag movement exhibited the lowest temperature. The Single-line movement involves repeatedly passing over the same path, leading to greater heat accumulation, whereas the Zigzag movement allows the laser to alternate along the weld line, distributing heat more evenly across the area, resulting in a lower maximum temperature. When considering the heated area, it was found that the Single-line movement caused heat distribution along the Y-axis from Y = -1 mm to Y = 1 mm, giving a heat spread radius of only 2 mm, which is smaller than the other movement patterns that spread heat from Y = -2 mm to Y = 2 mm. This is due to the fact that the Single-line movement does not alter the laser path along the Y-axis, resulting in heat accumulation along the same line, which leads to high temperatures and potential thermal damage to the tissue. The Line movement produced the second-highest maximum temperature, after the Single-line pattern, but had better heat distribution along the Y-axis. This makes the Line movement suitable for treatments that require high temperatures with broader heat distribution to cover a larger area of the wound. The Zigzag movement resulted in the lowest temperature during laser tissue welding but provided the most uniform heat distribution compared to the other movement patterns. The Zigzag laser movement is ideal for treatments where high temperatures are not desired, helping to minimize heat damage to surrounding tissue. This movement also ensures consistent heat distribution across the weld area, resulting in uniform treatment outcomes throughout the entire treatment region.

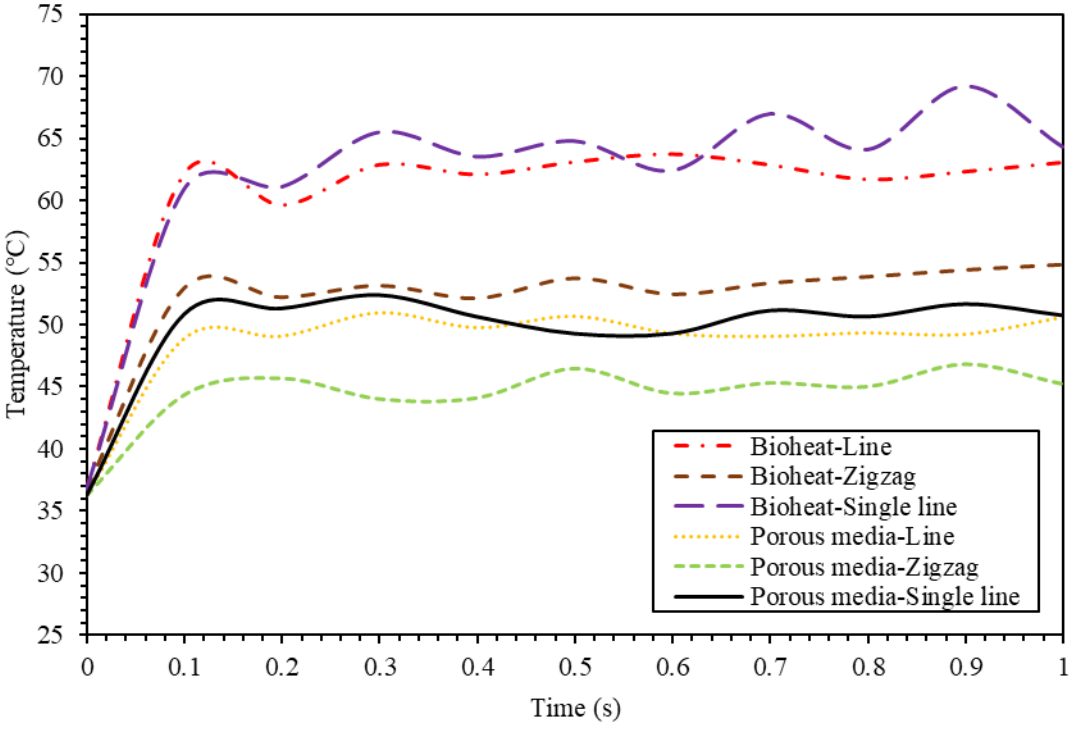


**Fig. 16** Comparison of the effect of maximum temperature when changing the laser movement pattern.

Figure 16 compares the maximum temperatures generated in Bioheat and Porous media models during laser tissue welding, considering three different laser movement patterns: Line, Zigzag, and Single-line. The results indicate that the Bioheat model with Single-line movement exhibited the highest maximum temperature, followed by the Bioheat model with Line movement, which showed a similar maximum temperature. In contrast, the Porous media model with Zigzag movement resulted in the lowest temperature. From animal tissue sample studies, it was found that the optimal temperature for wound welding should not exceed 65 °C, as temperatures higher than this threshold can cause thermal damage to the skin tissue. Conversely, temperatures below 45 °C are insufficient for proper tissue bonding. The ideal temperature for effective tissue welding is approximately 55 °C. Based on Fig. 16, the Bioheat model with Zigzag movement produced a maximum temperature closest to 55 °C, making it the most suitable for laser tissue welding. However, the temperature during welding also depends on the laser energy applied during the process.

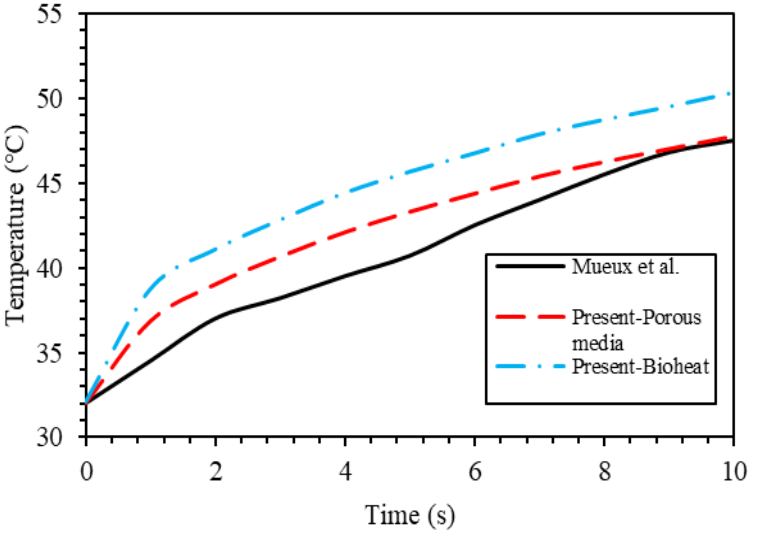


**Fig. 17** Comparing the results of the study with the experiments on animal tissue samples by Mueux *et al.*,[49] it was found that the Porus media model was more similar to the real experiments than the Bioheat model.

When the simulation results were compared with experimental results on real animal tissue, which is comparable to human skin tissue as studied by Mueux *et al.*,[49] as shown in Fig. 17, the parameters were adjusted to closely match the experimental conditions in the laboratory, it was found that the Porous media model produced temperatures closer to those observed in the real animal tissue than the Bioheat model. The animal tissue used in the experiments by Mueux is similar to human tissue; however, it does not include blood circulation, as is the case with living human tissue. Due to ethical constraints in experimental settings, this comparison may not fully represent the actual outcomes when applying this treatment method to living humans with active blood circulation. Nevertheless, the experimental findings can serve as a foundational basis for future studies aimed at improving accuracy to better reflect human tissue conditions.

## 4. Conclusion

This study focuses on developing a laser wound welding model. The 3D skin tissue simulation, based on the Bioheat and Porous media models, was conducted using a pulse laser heat source and three different movement patterns: Line, Zigzag, and Single Line. The results provide insights into constructing simulation models that more closely resemble real laboratory experiments. If successful, this research could reduce costs and resources for researchers studying laser wound welding, as accurate modeling will allow for faster and more precise research planning. In the future, this work could be further developed to aid in treatment planning. The results indicated that the Porous media model exhibited lower welding temperatures compared to the Bioheat model when the laser followed the same movement pattern. Among the movement patterns, the Single-line pattern resulted in the highest temperature, followed by the Line pattern, while the Zigzag pattern produced the lowest temperature. When comparing the accuracy of the models with real experiments, the Porous media model showed temperature values closer to the actual experimental results than the Bioheat model. In this study, a Rectangular Pulse Waveform was used for laser energy delivery. Future studies could explore the effects of different Pulse Waveforms, such as Triangular, Sawtooth, or Sine Pulse Waveforms, to further optimize the maximum temperature resulting from each laser movement pattern and tailor it to the specific characteristics of the wound being welded with the laser.

## Acknowledgments

This work was supported by the Thailand Science Research and Innovation Fundamental Fund fiscal year 2025 (TUFF43/2568), Graduate Studies Faculty of Engineering, Thammasat School of Engineering, Thammasat University Thailand and this study was supported by Thammasat University Research Fund, Contract No TUFT 35/2567"

## Conflict of Interest

There is no conflict of interest.

## Supporting Information

Not applicable.

## References

[1] Y. Chen, J. Huang, K. Wang, X. Li, Y. Rui, K. He, Experimental research on mechanism of collagen remodeling and excellent properties of skin incisions under dual beam laser welding, *Optics & Laser Technology*, 2024, **169**, 110168, doi: 10.1016/j.optlastec.2023.110168.

[2] Y. Chen, J. Huang, S. Xia, K. Wang, Y. Rui, Effect of laser energy on protein conformation and lipid structure in skin tissue, *Optics & Laser Technology*, 2023, **160**, 109077, doi: 10.1016/j.optlastec.2022.109077.

[3] C. Li, J. Huang, M. Zhang, Y. Chen, T. Liu, K. Wang, Effect of preloading force on capability of laser welding for skin tissue, *Optics and Lasers in Engineering*, 2023, **165**, 107538, doi: 10.1016/j.optlaseng.2023.107538.

[4] P. Wongchadakul, P. Rattanadecho, K. Jiamjiroch, Experimental analysis of thermal transport in low-level laser therapy on skin tissue: the influence on therapeutic efficacy, pain sensation and dry skin wound, *International Journal of Thermal Sciences*, 2024, **199**, 108886, doi: 10.1016/j.ijthermalsci.2024.108886.

[5] N. Salma, M. Wang-Evers, D. Karasik, A. Yerevanian, H. Downs, T. Luo, A. E. Doyle, Z. Tannous, J. M. Cacicedo, D. Manstein, Large area fractional laser treatment of mouse skin increases energy expenditure, *iScience*, 2024, **27**, 108677, doi: 10.1016/j.isci.2023.108677.

[6] S. A. Razack, Y. Lee, H. Shin, S. Duraiarasan, B.-S. Chun, H. W. Kang, Cellulose nanofibrils reinforced chitosan-gelatin based hydrogel loaded with nanoemulsion of oregano essential oil for diabetic wound healing assisted by low level laser therapy, *International Journal of Biological Macromolecules*, 2023, **226**, 220-239, doi: 10.1016/j.ijbiomac.2022.12.003.

[7] A. Priyadarshi, G. K. Keshri, A. Gupta, Dual-NIR wavelength (pulsed 810nm and superpulsed 904nm lasers) photobiomodulation therapy synergistically augments full-thickness burn wound healing: a non-invasive approach, *Journal of Photochemistry and Photobiology B: Biology*, 2023, **246**, 112761, doi: 10.1016/j.jphotobiol.2023.112761.

[8] M. E. Lou, M. D. Kleinhenz, R. Schroeder, K. Lechtenberg, S. Montgomery, J. F. Coetzee, A. V. Viscardi, Evaluating the utility of a $CO_2$ surgical laser for piglet tail docking to reduce behavioral and physiological indicators of pain and to improve wound healing: a pilot study, *Applied Animal Behaviour Science*, 2022, **254**, 105720, doi: 10.1016/j.applanim.2022.105720.

[9] W. He, J. Frueh, J. Shao, M. Gai, N. Hu, Q. He, Guidable GNR-$Fe_3O_4$-PEM@$SiO_2$ composite particles containing near infrared active nanocalorifiers for laser assisted tissue welding, *Colloids and Surfaces A: Physicochemical and Engineering Aspects*, 2016, **511**, 73-81, doi: 10.1016/j.colsurfa.2016.09.052.

[10] H. Guo, X. Zhang, H. Li, C. Fu, L. Jiang, Y. Hu, J. Huang, J. Chen, Q. Zeng, Dynamic panoramic presentation of skin function after fractional $CO_2$ laser treatment, *Iscience*, 2023, **26**, 107559, doi: 10.1016/j.isci.2023.107559.
[11] Y. Chen, J. Huang, S. Xia, K. Wang, Y. Rui, Evaluation of fusion performances of skin wound incisions under different defocus amounts in laser tissue welding, *Optics & Laser Technology*, 2023, **165**, 109570, doi: 10.1016/j.optlastec.2023.109570.
[12] M. Belfort, Z. Bateni, D. M. Haydel, M. Larson, Y. Wadia, A. A. Shamshirsaz, W. Whitehead, Evaluation of the effects of laser tissue welding on the spinal cord and skin in a 30 day study of simulated spina bifida repair in rabbits, *American Journal of Obstetrics and Gynecology*, 2017, **216**, S60, doi: 10.1016/j.ajog.2016.11.971.
[13] H. H. Pennes, Analysis of tissue and arterial blood temperatures in the resting human forearm, *Journal of Applied Physiology*, 1998, **85**, 5-34, doi: 10.1152/jappl.1998.85.1.5.
[14] Q. Zhang, Y. Sun, J. Yang, A. K. Soh, X. Wang, Theoretical analysis of thermal response in biological skin tissue subjected to multiple laser beams, *Case Studies in Thermal Engineering*, 2021, **24**, 100853, doi: 10.1016/j.csite.2021.100853.
[15] Q. Zhang, Y. Sun, J. Yang, Thermoelastic behavior of skin tissue induced by laser irradiation based on the generalized dual-phase lag model, *Journal of Thermal Biology*, 2021, **100**, 103038, doi: 10.1016/j.jtherbio.2021.103038.
[16] P. Wongchadakul, P. Rattanadecho, T. Wessapan, Simulation of temperature distribution in different human skin types exposed to laser irradiation with different wavelengths and laser irradiation intensities, *Songklanakarin Journal of Science and Technology*, 2019, **41**, 529-538.
[17] P. Wongchadakul, P. Rattanadecho, T. Wessapan, Implementation of a thermomechanical model to simulate laser heating in shrinkage tissue (effects of wavelength, laser irradiation intensity, and irradiation beam area), *International Journal of Thermal Sciences*, 2018, **134**, 321-336, doi: 10.1016/j.ijthermalsci.2018.08.008.
[18] R. Singh, K. Das, J. Okajima, S. Maruyama, S. C. Mishra, Modeling skin cooling using optical windows and cryogens during laser induced hyperthermia in a multilayer vascularized tissue, *Applied Thermal Engineering*, 2015, **89**, 28-35, doi: 10.1016/j.applthermaleng.2015.06.006.
[19] S. M. Seyedpour, M. Azhdari, L. Lambers, T. Ricken, G. Rezazadeh, One-dimensional thermomechanical bio-heating analysis of viscoelastic tissue to laser radiation shapes, *International Journal of Heat and Mass Transfer*, 2024, **218**, 124747, doi: 10.1016/j.ijheatmasstransfer.2023.124747.
[20] J. Saemathong, N. Pannucharoenwong, V. Mongkol, S. Vongpradubchai, P. Rattanadecho, Analyzing two laser thermal energy calculation equations: a comparison of beer-lambert's law and light transport equation, *Engineered Science*, 2023, **24**, 912, doi: 10.30919/es912.
[21] P. Kishore, S. Kumar, V. M. Patel, Conjugate heat transfer analysis of laser-irradiated cylindrical-shaped biological tissue embedded with the optical inhomogeneity, *International Communications in Heat and Mass Transfer*, 2022, **137**, 106302, doi: 10.1016/j.icheatmasstransfer.2022.106302.
[22] K. Chen, Y. Liang, W. Zhu, X. Sun, T. Wang, Simulation of temperature distribution in skin under laser irradiation with different wavelengths, *Optik*, 2014, **125**, 1676-1679, doi: 10.1016/j.ijleo.2013.10.021.
[23] P. Wongchadakul, A. K. Datta, P. Rattanadecho, Natural convection effects on heat transfer in a porous tissue in 3-D radiofrequency cardiac ablation, *International Journal of Heat and Mass Transfer*, 2023, **204**, 123832, doi: 10.1016/j.ijheatmasstransfer.2022.123832.
[24] P. Rattanadecho, P. Keangin, Numerical study of heat transfer and blood flow in two-layered porous liver tissue during microwave ablation process using single and double slot antenna, *International Journal of Heat and Mass Transfer*, 2013, **58**, 457-470, doi: 10.1016/j.ijheatmasstransfer.2012.10.043.
[25] S. Pongpakpien, W. Preechaphonkul, P. Rattanadecho, Effects of thermal and electrical properties on porous liver during microwave ablation using microwave coaxial slot antenna, *International Journal of Heat and Technology*, 2020, **38**, 361-370, doi: 10.18280/ijht.380211.
[26] B. Li, L. Zhang, B. Shang, Y. Huo, Numerical investigation on heat transfer characteristics in battery thermal management with phase change material composited by toroidal porous medium, *International Communications in Heat and Mass Transfer*, 2024, **154**, 107414, doi: 10.1016/j.icheatmasstransfer.2024.107414.
[27] M. Iasiello, A. Andreozzi, N. Bianco, K. Vafai, The porous media theory applied to radiofrequency catheter ablation, *International Journal of Numerical Methods for Heat & Fluid Flow*, 2020, **30**, 2669-2681, doi: 10.1108/hff-11-2018-0707.
[28] J. M. Huyghe, T. Arts, D. H. van Campen, R. S. Reneman, Porous medium finite element model of the beating left ventricle, *American Journal of Physiology-Heart and Circulatory Physiology*, 1992, **262**, H1256-H1267, doi: 10.1152/ajpheart.1992.262.4.h1256.
[29] L. Zhang, X. Shang, An integral transform solution for bioheat transfer in skin tissue subjected to surface laser irradiation, *International Journal of Heat and Mass Transfer*, 2021, **180**, 121706, doi: 10.1016/j.ijheatmasstransfer.2021.121706.
[30] B. Partovi, H. Ahmadikia, M. Mosharaf-Dehkordi, Analytical and numerical analysis of the dual-pulse lag heat transfer in a three-dimensional tissue subjected to a moving multi-point laser beam, *Journal of Thermal Biology*, 2023, **112**, 103431, doi: 10.1016/j.jtherbio.2022.103431.
[31] A. Kabiri, M. R. Talaee, Thermal field and tissue damage analysis of moving laser in cancer thermal therapy, *Lasers in Medical Science*, 2021, **36**, 583-597, doi: 10.1007/s10103-020-03070-7.
[32] Y. Hu, X.-Y. Zhang, X.-F. Li, Thermoelastic analysis of biological tissue during hyperthermia treatment for moving laser heating using fractional dual-phase-lag bioheat conduction, *International Journal of Thermal Sciences*, 2022, **182**, 107806, doi: 10.1016/j.ijthermalsci.2022.107806.
[33] T. Chabuanoi, N. Pannucharoenwong, P. Wongsangnoi, P.

Rattanadecho, J. Saemathong, S. Hemathulin, Simulation effect of laser moving speed and spot size on maximum temperature in laser welding human skin tissue, *Engineered Science*, 2024, **31**, 1193, doi: 10.30919/es1193.
[34] C. Li, K. Wang, Effect of welding temperature and protein denaturation on strength of laser biological tissues welding, *Optics & Laser Technology*, 2021, **138**, 106862, doi: 10.1016/j.optlastec.2020.106862.
[35] S. Wray, M. Cope, D. T. Delpy, J. S. Wyatt, E. O. R. Reynolds, Characterization of the near infrared absorption spectra of cytochrome aa3 and haemoglobin for the non-invasive monitoring of cerebral oxygenation, *Biochimica et Biophysica Acta (BBA) - Bioenergetics*, 1988, **933**, 184-192, doi: 10.1016/0005-2728(88)90069-2.
[36] S. H. Tseng, P. Bargo, A. Durkin, N. Kollias, Chromophore concentrations, absorption and scattering properties of human skin *in-vivo*, *Optics Express*, 2009, **17**, 14599, doi: 10.1364/oe.17.014599.
[37] H. O. Tabakoglu, N. Topaloglu, M. Gulsoy, The effect of irradiance level in 980-nm diode laser skin welding, *Photomedicine and Laser Surgery*, 2010, **28**, 453-458, doi: 10.1089/pho.2009.2569.
[38] A. Bhowmik, R. Repaka, S. C. Mishra, K. Mitra, Thermal assessment of ablation limit of subsurface tumor during focused ultrasound and laser heating, *Journal of Thermal Science and Engineering Applications*, 2016, **8**, 011012, doi: 10.1115/1.4030731.
[39] G. Aguilar, B. Majaron, J. A. Viator, B. Basinger, E. Karapetian, L. O. Svaasand, E. J. Lavernia, J. S. Nelson, Influence of spraying distance and postcooling on cryogen spray cooling for dermatologic laser surgery, *SPIE - The International Society for Optical Engineering*, 2001, **4244**, 82-92, doi: 10.1117/12.427778.
[40] G. Aguilar, S. H. Díaz, E. J. Lavernia, J. S. Nelson, Cryogen spray cooling efficiency: improvement of port wine stain laser therapy through multiple-intermittent cryogen spurts and laser pulses, *Lasers in Surgery and Medicine*, 2002, **31**, 27-35, doi: 10.1002/lsm.10076.
[41] H. Piazena, H. Meffert, R. Uebelhack, Spectral remittance and transmittance of visible and infrared-a radiation in human skin-comparison between in vivo measurements and model calculations, *Photochemistry and photobiology*, 2017, **93**, 1449-1461, doi: 10.1111/php.12785.
[42] A. R. A. Khaled, K. Vafai, The role of porous media in modeling flow and heat transfer in biological tissues, *International Journal of Heat and Mass Transfer*, 2003, **46**, 4989-5003, doi: 10.1016/s0017-9310(03)00301-6.
[43] H. C. Brinkman, On the permeability of media consisting of closely packed porous particles, *Flow, Turbulence and Combustion*, 1949, **1**, 81-86, doi: 10.1007/BF02120318.
[44] K. Vafai, Convective flow and heat transfer in variable-porosity media, *Journal of Fluid Mechanics*, 1984, **147**, 233, doi: 10.1017/s002211208400207x.
[45] M. Motamedi, A. Gonzales, G. Yoon, A. J. Welch, Thermal response of gastro-intestinal tissue to Nd-Yag laser irradiation: A theoretical and experimental investigation, *International Congress on Applications of Lasers & Electro-Optics*, 1983, **37**, 80-89, doi: 10.2351/1.5057464.
[46] A. Welch, The thermal response of laser irradiated tissue, *IEEE Journal of Quantum Electronics*, 1984, **20**, 1471-1481, doi: 10.1109/JQE.1984.1072339.
[47] J. Saemathong, N. Pannucharoenwong, V. Mongkol, S. Vongpradubchai, P. Rattanadecho, Analyzing two laser thermal energy calculation equations: a comparison of beer-lambert's law and light transport equation, *Engineered Science*, 2023, **24**, 912, doi: 10.30919/es912.
[48] J. Ma, X. Yang, S. Liu, Y. Sun, J. Yang, Exact solution of thermal response in a three-dimensional living bio-tissue subjected to a scanning laser beam, *International Journal of Heat and Mass Transfer*, 2018, **124**, 1107-1116, doi: 10.1016/j.ijheatmasstransfer.2018.04.042.
[49] N. Museux, L. Perez, L. Autrique, D. Agay, Skin burns after laser exposure: Histological analysis and predictive simulation, *Burns*, 2012, **38**, 658-667, doi: 10.1016/j.burns.2011.12.006.